Supplement of Hydrol. Earth Syst. Sci., 28, 2969–2989, 2024
https://doi.org/10.5194/hess-28-2969-2024-supplement

Hydrology and Earth System Sciences
Open Access
EGU

Supplement of

Assessing the impact of climate change on high return levels of peak flows in Bavaria applying the CRCM5 large ensemble

Florian Willkofer et al.

Correspondence to: Florian Willkofer (florian.willkofer@lmu.de, florian.willkofer@campus.lmu.de)

Supplements

S1. CanESM2 Large Ensemble

The first link is the Canadian Earth System Model, version 2 (CanESM2) large ensemble (LE) produced by the Canadian Centre for Climate Modelling and analysis (CCCma) (Fyfe et al., 2017; Kirchmeier-Young et al., 2017; Arora et al., 2011; Leduc et al., 2019). This large ensemble comprises 50 independent members from 1950 to 2100 with a spatial resolution of ~2.81° representing the internal (or natural) variability of the climate system by altering initial conditions, thus without changing the model structure or physics (Kirchmeier-Young et al., 2017; Fyfe et al., 2017). At first, a five member historical ensemble has been established initialized by 1000 iterations of a one-year equilibrium run of 1850 with preindustrial forcings (Kirchmeier-Young et al., 2017; Arora et al., 2011; Leduc et al., 2019). Within the timespan from 1850 to 2005, these members were forced by atmospheric changes, variability of the solar cycle, and explosive volcanoes, differing only in their initial state of cloud-overlap values (Leduc et al., 2019; Arora et al., 2011). Each of the five historical runs was further expanded from 1950 to 2100 by ten members through alterations of the initial cloud parameters (Leduc et al., 2019; Kirchmeier-Young et al., 2017; Fyfe et al., 2017; Sigmond et al., 2018). While natural and anthropogenic forcings were employed for the historical part of the members (1950 through 2005), the representative concentration pathway 8.5 (RCP8.5, van Vuuren et al. (2011)) emission scenario forced the simulations from 2006 and beyond (Kirchmeier-Young et al., 2017; Leduc et al., 2019; Fyfe et al., 2017; Sigmond et al., 2018).

The mismatch of spatial resolution between model outputs from the CanESM2-LE (~2.81° ≈ 310 km) and the hydrological model scale (500 m x 500 m) is likely to affect modelling results of the later. Thus, two common downscaling approaches (dynamical and statistical) were utilized consecutively to enhance the spatial resolution and foster the applicability for hydrological modelling.

S2. CRCM5 Large Ensemble

The Canadian Regional Climate Model, version 5 (CRCM5; Martynov et al., 2013; Šeparović et al., 2013) was employed by the Ouranos Consortium on Regional Climatology and Adaptation to Climate Change to dynamically downscale the CanESM2-LE to 0.11° (~12 km) over two domains (Europe (EU) and northeastern North America (NNA)) for the available period from 1950 through 2099 and emission scenarios (historical until 2005, RCP8.5 from 2006 to 2100) (Leduc et al., 2019). These 50 transient simulations of the CRCRM5 Large Ensemble (CRCM5-LE; Leduc et al., 2019, data available at www.climex-project.org) provide the basis to assess the impact of climate change on hydro-meteorological extreme events for Bavaria and Québec. A comparison between the

CRCM5-LE and the E-OBS observational gridded dataset (Haylock et al., 2008) at the CRCM5 grid revealed biases for a historical period between 1980 and 2012 which show regional and seasonal variations in magnitude over Europe (Leduc et al., 2019). Within the study area of the hydrological Bavaria, a cold bias of down to -2 °C is dominant for long term mean air temperature values in all seasons but winter, where biases vary merely around zero (-1 °C to +1 °C). However, mountainous regions of the Alps and Alpine foreland exhibit a warm bias of up to +4 °C. Mean precipitation sums show a systematic wet bias throughout the year (Leduc et al., 2019), ranging from 1 to 2 mm d^{-1} in shallow areas and 2 to 4 mm d^{-1} in mountainous regions of the hydrological Bavaria, whereupon the larger bias occurs in winter.

Since this study focuses on high return levels of fluvial flood events, high intensity precipitation events of at least daily duration are important (Berghuijs et al., 2019; Keller et al., 2018; Merz and Blöschl, 2003). Hence, an adequate representation of these events in the historical or reference period of the RCMs compared to observations fosters the acceptance for impact studies. For our study area a comparison of moderate precipitation extremes of 10-year return levels between the RCM output and observations by Poschlod et al. (2021) revealed that differences in precipitation intensities of the RCM with a duration of 24 hours exhibit a slight overestimation north of the Alps (most of the areas below +20 %) and a smaller underestimation in the Alps (most parts above -10 %).

For further details on the performance of the CRCM5-LE over the respective domains and projected changes the reader is referred to Leduc et al. (2019) and Poschlod et al. (2021).

S3. Bias correction

The biases in precipitation and air temperature of the CRCM5-LE during the historical period cannot be ignored within the study area, as they are supposed to affect the hydrological cycle simulated by the hydrological model (Poschlod et al., 2020; Maraun, 2016; Ehret et al., 2012; Teutschbein and Seibert, 2012). Thus, a quantile-mapping approach after Mpelasoka and Chiew (2009) (daily translation) was used to adjust the CRCM5-LE outputs required for the hydrological simulations (precipitation, 2 m air temperature, relative humidity, surface wind speed, surface downwelling shortwave radiation) at the RCM scale. Therefore, the high resolution sub-daily climate reference (SDCLIREF; 500 m x 500 m, 3-hourly data; not published) was aggregated to the RCM grid by mass conservative remapping. Adjustments to the original approach (i.e., multiplicative and additive correction factors for variables other than precipitation (Willkofer et al., 2018), 3-hourly correction factors for every quantile bin and each month) allowed for its application to sub-daily data and a single set of correction factors derived from all 50 members of the ensemble was used for the adjustment of each member. To preserve the inter-member variability (i.e., natural variability) all 50 members were pooled for the determination of quantiles and correction factors before the

correction factors were subsequently applied to each individual ensemble separately. To account for seasonally varying biases correction factors were determined for each month, and to account for diurnal biases each 3h timestep (Brunner et al., 2021; Poschlod et al., 2020). Prior to the bias correction of precipitation, the ratio of wet to dry days of the RCM was adjusted to match the ratio of the observations by removing the 'drizzle' (insignificantly small precipitation values originating from the coarse scale of the RCM; Dettinger et al., 2004; Maraun, 2016). Since precipitation values below 1 mm d^{-1} do not significantly contribute to the overall precipitation sum (Dai, 2001) and this value is considered a standardized threshold (Kjellström et al., 2010; Maraun, 2016), we applied this threshold to the RCM precipitation data.

The quantile mapping approach is a common and frequently used method to adjust RCM outputs to match long term statistics of the observations as it often provides better adaptation to the observations than other methods and is applicable to climatic variables other than precipitation (Teutschbein and Seibert, 2012; Themeßl et al., 2011). However, this approach – as well as other bias adjustment methods – affects the distribution leading to changes in extreme values and consequently in altered climate change signals (Willkofer et al., 2018; Ehret et al., 2012; Maraun, 2016). This effect must be considered for the interpretation and discussion of the results. Furthermore, biases are further assumed to be stationary in space and time (Teutschbein and Seibert, 2012).

S4. The hydrological model setup and performance

A semi-global and semi-automated calibration approach employing globally defined parameters for spatially distributed parameters (manual calibration) and locally set parameters for soil storage components (automated calibration) at each gauge (Willkofer et al., 2020). This approach aims to reduce the effects of overparameterization and equifinality conceding a reduction in goodness of fit of modeled discharge values at some gauges due to possible misrepresentation of certain catchment characteristics. The Figure 1 shows the model performance as illustrated in Willkofer et al. (2020) and Poschlod et al. (2020), a) showing NSE and b) showing KGE values at each of the 98 gauges (one gauge not depicting any values due to missing observations).

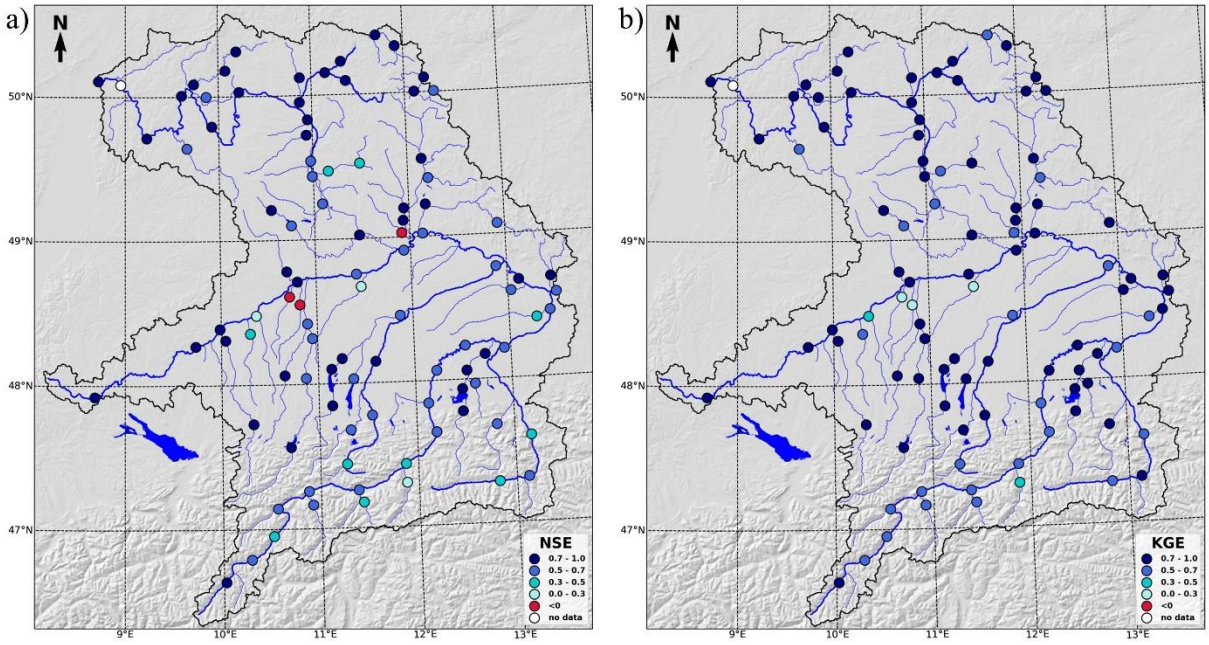

Figure S1: Performance of the hydrological model for each of the 98 gauges. a) showing the NSE, b) showing the KGE as presented in Willkofer et al. (2020).

The level of trust (LOT) depicts a quality measure for each gauge for the representation of high flows with certain return levels (HF_T). It is calculated as the absolute value of the relative difference between the HF_T derived from observed and modeled discharge. The HF_T was calculated applying the Generalized Pareto Distribution (GPD) on 30-year time series of both datasets from 1981 to 2010, employing the L-Moments (LM) approach for parameter estimation. Figure 2 shows the LOT for the HF_{20} as presented in Willkofer et al. (2020).

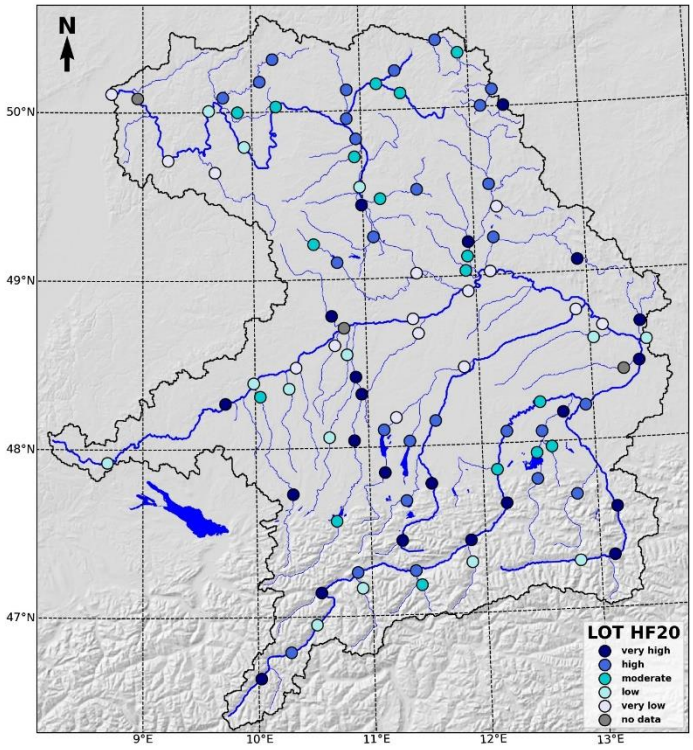

Figure S2: LOT of the HF_{20} derived from observed and modelled discharge as presented in Willkofer et al. (2020)

S5. Benefit of hydro-SMILE

In Figure 3, a comparison is made between the HF_{100} estimates derived using the empirical probability of non-exceedance and those obtained using the GEV distribution (and associated 95 % confidence intervals) for the entire ensemble of 1,500 AM values. The robust values obtained from the empirical probability are used as the benchmark for this comparison.

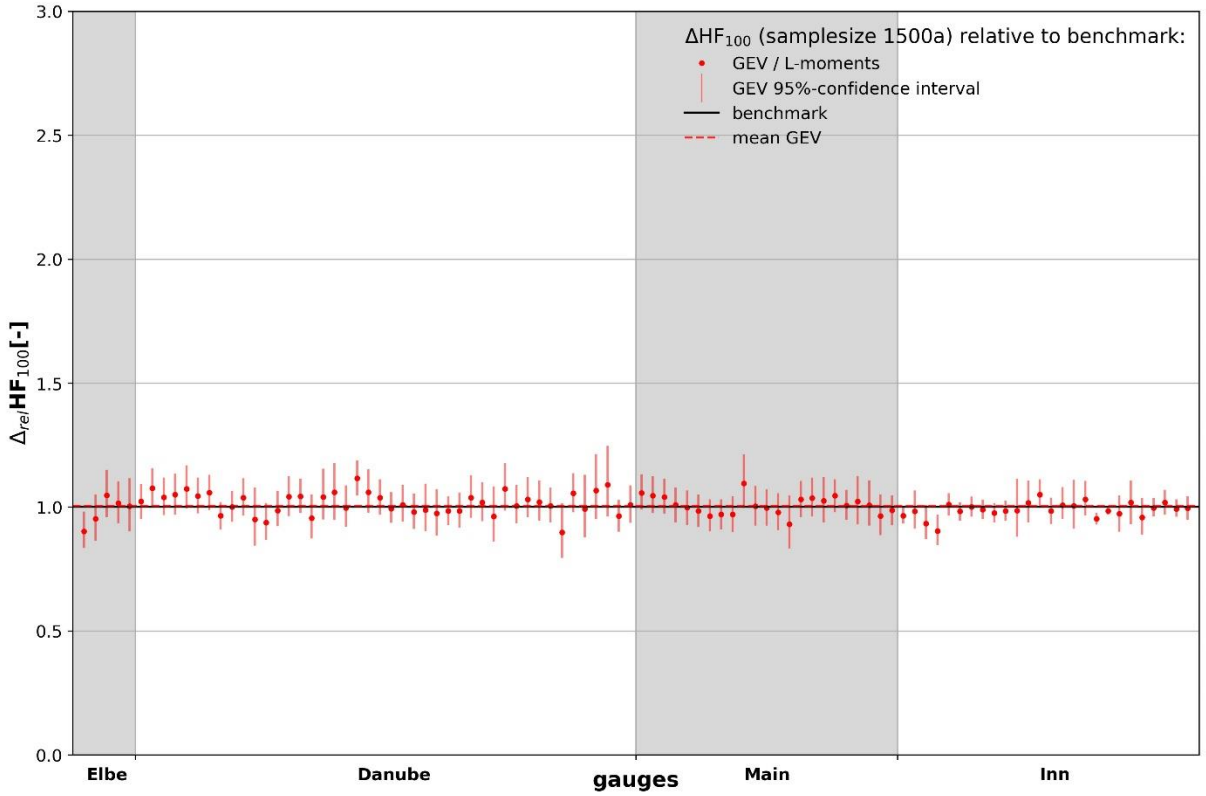

Figure S3: Relative difference of the HF_{100} values (red dots) and respective 95th confidence intervals (vertical red lines) calculated using the GEV distribution from the benchmark HF_{100} value (black solid line) derived from the probability of non-exceedance p = 0.01. The results gained by the GEV distribution are based on the entire reference database of 1500 AM values for each of the 98 gauges. The horizontal red dashed line illustrates the mean of the relative difference of the HF_{100} calculated using the GEV distribution for all 98 gauges.

The estimates obtained using the GEV show differences from the benchmark, with varying magnitudes across the gauges. However, the mean difference across all HF_{100} estimates is small and marginally different from the benchmark. For most gauges, the individual differences from the benchmark are also small, with only two gauges showing values exceeding ±10%. However, for 7 of 98 gauges the 95 % confidence interval does not overlap with the benchmark, indicating that in this case the empirical approach yields a more robust value compared to the GEV estimates even with the enhanced robustness gained by employing 1,500 AM values as a sample. However, if the unknown population could be represented by the GEV, the distribution would yield a better fit. Therefore, the determination of peak flows with extreme return periods employing the empirical probability on the vast data base of a hydro-SMILE allows for a more precise estimation. Hence, also the estimation of future return periods is more

robust allowing for a better quantification of the changing dynamics in the frequency and intensity of high return periods in future projections due to changes in the climate.

S6. Dynamics in HF_{100} frequency and magnitude

Figure 4 show the spatial distribution of the changes in HF_{100} frequency (a) and magnitude (b) between the reference period and the far future period (2070-2099).

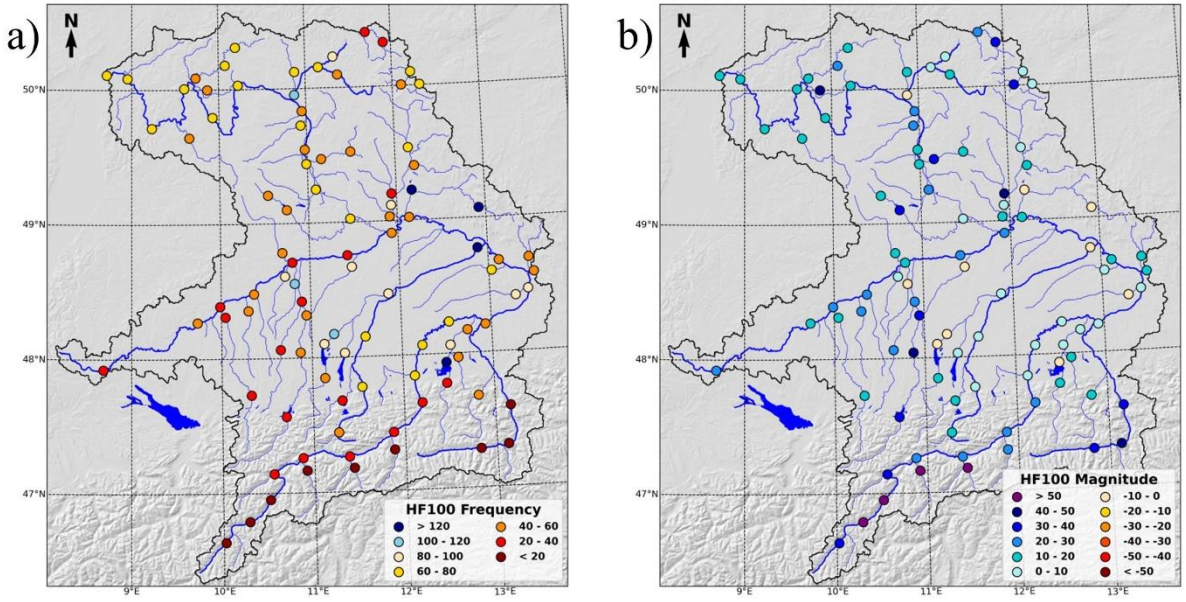

Figure S4: Maps showing the spatial distribution of the dynamics in HF_{100} frequency (a) and magnitude (b) for the far future periods from 2070 to 2099.

References

Arora, V. K., Scinocca, J. F., Boer, G. J., Christian, J. R., Denman, K. L., Flato, G. M., Kharin, V. V., Lee, W. G., and Merryfield, W. J.: Carbon emission limits required to satisfy future representative concentration pathways of greenhouse gases, Geophys. Res. Lett., 38, L05805, doi:10.1029/2010GL046270, 2011.

Berghuijs, W. R., Harrigan, S., Molnar, P., Slater, L. J., and Kirchner, J. W.: The Relative Importance of Different Flood-Generating Mechanisms Across Europe, Water Resour. Res., doi:10.1029/2019WR024841, 2019.

Brunner, M. I., Slater, L., Tallaksen, L. M., and Clark, M.: Challenges in modeling and predicting floods and droughts: A review, WIREs Water, 8, doi:10.1002/wat2.1520, 2021.

Dai, A.: Global Precipitation and Thunderstorm Frequencies. Part II: Diurnal Variations, J. Climate, 14, 1112–1128, doi:10.1175/1520-0442(2001)014%3C1112:GPATFP%3E2.0.CO;2, 2001.

Dettinger, M. D., Cayan, D. R., Meyer, M. K., and Jeton, A. E.: Simulated Hydrologic Responses to Climate Variations and Change in the Merced, Carson, and American River Basins, Sierra Nevada, California, 1900–2099, Climatic Change, 62, 283–317, doi:10.1023/B:CLIM.0000013683.13346.4f, 2004.

Ehret, U., Zehe, E., Wulfmeyer, V., Warrach-Sagi, K., and Liebert, J.: HESS Opinions "Should we apply bias correction to global and regional climate model data?", Hydrol. Earth Syst. Sci., 16, 3391–3404, doi:10.5194/hess-16-3391-2012, 2012.

Fyfe, J. C., Derksen, C., Mudryk, L., Flato, G. M., Santer, B. D., Swart, N. C., Molotch, N. P., Zhang, X., Wan, H., Arora, V. K., Scinocca, J., and Jiao, Y.: Large near-term projected snowpack loss over the western United States, Nature communications, 8, 14996, doi:10.1038/ncomms14996, 2017.

Haylock, M. R., Hofstra, N., Klein Tank, A. M. G., Klok, E. J., Jones, P. D., and New, M.: A European daily high-resolution gridded data set of surface temperature and precipitation for 1950–2006, J. Geophys. Res., 113, doi:10.1029/2008JD010201, 2008.

Keller, L., Rössler, O., Martius, O., and Weingartner, R.: Delineation of flood generating processes and their hydrological response, Hydrol. Process., 32, 228–240, doi:10.1002/hyp.11407, 2018.

Kirchmeier-Young, M. C., Zwiers, F. W., and Gillett, N. P.: Attribution of Extreme Events in Arctic Sea Ice Extent, J. Climate, 30, 553–571, doi:10.1175/JCLI-D-16-0412.1, 2017.

Kjellström, E., Boberg, F., Castro, M., Christensen, J. H., Nikulin, G., and Sánchez, E.: Daily and monthly temperature and precipitation statistics as performance indicators for regional climate models, Clim. Res., 44, 135–150, doi:10.3354/cr00932, 2010.

Leduc, M., Mailhot, A., Frigon, A., Martel, J.-L., Ludwig, R., Brietzke, G. B., Giguère, M., Brissette, F., Turcotte, R., Braun, M., and Scinocca, J.: The ClimEx Project: A 50-Member Ensemble of Climate Change Projections at 12-km Resolution over Europe and Northeastern North America with the Canadian Regional Climate Model (CRCM5), Journal of Applied Meteorology and Climatology, 58, 663–693, doi:10.1175/JAMC-D-18-0021.1, 2019.

Maraun, D.: Bias Correcting Climate Change Simulations - a Critical Review, Curr Clim Change Rep, 2, 211–220, doi:10.1007/s40641-016-0050-x, 2016.

Martynov, A., Laprise, R., Sushama, L., Winger, K., Šeparović, L., and Dugas, B.: Reanalysis-driven climate simulation over CORDEX North America domain using the Canadian Regional Climate Model, version 5: model performance evaluation, Clim Dyn, 41, 2973–3005, doi:10.1007/s00382-013-1778-9, 2013.

Merz, R. and Blöschl, G.: A process typology of regional floods, Water Resour. Res., 39, doi:10.1029/2002WR001952, 2003.

Mpelasoka, F. S. and Chiew, F. H. S.: Influence of Rainfall Scenario Construction Methods on Runoff Projections, Journal of Hydrometeorology, 10, 1168–1183, doi:10.1175/2009JHM1045.1, 2009.

Poschlod, B., Ludwig, R., and Sillmann, J.: Ten-year return levels of sub-daily extreme precipitation over Europe, Earth Syst. Sci. Data, 13, 983–1003, doi:10.5194/essd-13-983-2021, 2021.

Poschlod, B., Willkofer, F., and Ludwig, R.: Impact of Climate Change on the Hydrological Regimes in Bavaria, Water, 12, 1599, doi:10.3390/w12061599, 2020.

Šeparović, L., Alexandru, A., Laprise, R., Martynov, A., Sushama, L., Winger, K., Tete, K., and Valin, M.: Present climate and climate change over North America as simulated by the fifth-generation Canadian regional climate model, Clim Dyn, 41, 3167–3201, doi:10.1007/s00382-013-1737-5, 2013.

Sigmond, M., Fyfe, J. C., and Swart, N. C.: Ice-free Arctic projections under the Paris Agreement, Nature Clim Change, 8, 404–408, doi:10.1038/s41558-018-0124-y, 2018.

Teutschbein, C. and Seibert, J.: Bias correction of regional climate model simulations for hydrological climate-change impact studies: Review and evaluation of different methods, Journal of Hydrology, 456-457, 12–29, doi:10.1016/j.jhydrol.2012.05.052, 2012.

Themeßl, M. J., Gobiet, A., and Leuprecht, A.: Empirical-statistical downscaling and error correction of daily precipitation from regional climate models, Int. J. Climatol., 31, 1530–1544, doi:10.1002/joc.2168, 2011.

van Vuuren, D. P., Edmonds, J., Kainuma, M., Riahi, K., Thomson, A., Hibbard, K., Hurtt, G. C., Kram, T., Krey, V., Lamarque, J.-F., Masui, T., Meinshausen, M., Nakicenovic, N., Smith, S. J., and Rose, S. K.: The representative concentration pathways: an overview, Climatic Change, 109, 5–31, doi:10.1007/s10584-011-0148-z, 2011.

Willkofer, F., Schmid, F.-J., Komischke, H., Korck, J., Braun, M., and Ludwig, R.: The impact of bias correcting regional climate model results on hydrological indicators for Bavarian catchments, Journal of Hydrology: Regional Studies, 19, 25–41, doi:10.1016/j.ejrh.2018.06.010, 2018.

Willkofer, F., Wood, R. R., Trentini, F. von, Weismüller, J., Poschlod, B., and Ludwig, R.: A Holistic Modelling Approach for the Estimation of Return Levels of Peak Flows in Bavaria, Water, 12, 2349, doi:10.3390/w12092349, 2020.